Plant Archives Vol. 17 No. 2, 2017 pp. 825-832 *ISSN 0972-5210*

THERMAL STUDIES OF PURE AND DOPED CDS NANOPARTICLES

S. Rinu Sam

Sivaji College of Engineering and Technology, Manivila (Tamil Nadu), India.
E-mail : r.sam0003@yahoo.co.in

Abstract

Semiconductor nanoparticles doped with transition metal ions have attracted wide attention due to their excellent luminescent properties. The transition metal ions doped nanoparticles show different optical properties corresponding to their host counter parts. These nanoparticles have found tremendous applications in optical light emitting diodes. Among the family of II–VI semiconductor CdS is the foremost candidates because of their favourable electronic and optical properties for optoelectronic applications. The synthesis of pure CdS nano particles and CdS doped with transition metal ions (Zn^{2+},Mn^{2+},Cu^{2+}) were done by microwave assisted solvothermal method. XRD studies revels that CdS nanocrystals in cubic as well as hexagonal phase. The obtained nanomaterials have been characterised by Scanning Electron Microscopy (SEM) and the thermal analysis of DSC and TGA.

Key words: Nanoparticles, solvothermal, doped, XRD, SEM, DSC, TGA.

Introduction

Nanocrystalline semiconductor have been intensively investigated over the past years due to their specific optic, electronic and catalytic properties (1-6). All these properties attributed from the high surface to volume ratio and the size quantization effect. II–VI group semiconductor nanomaterials are great interest in the field of optics due to their strongly size dependent optical properties (7). Numerous methods have been developed for the fabrication of such semiconductor nanomaterials (8–12) including chemical reduction, liquid reaction method, sacrificial template method, hydro thermal and solvothemal method. (13-19) amoung all these methods, recently the solvothermal method has potential advantages of relatively low cost, uniform size, high purity and controlled morphology. (17-19) In this method, solvents are the key issue for the preparation of CdS nanoparticles under solvothermal condition. Mixed solutions are used in order to obtain excellent semiconductor CdS nanoparticles.

Expermental

Ethylene glycol ($HOCH_2CH_2OH$), thioacetamide (CH_3CSNH_2) and cadmium acetate (Cd (CH_3COO)2. $2H_2O$] are the analytical reagents. In this present investigation ethylene glycol was used as the solvent. Thioacetamide and cadmium acetate were added 1:1 ratio mixed with 30 ml of ethylene glycol and to get a clear transparent solution, the above mixture is stirred well at room temperature. The solution was subjected to microwave irradiation of 800 W for 20 minutes. Thioacetamide can react with the trace water containing in ethylene glycol and also with cadmium acetate, and releases H_2S gradually. From the productive mixture The precipitate of orange coloured CdS nanocrystallites were separated out and washed with de-ionized water for four times and then with alcohol twice. The CdS nanoparticles were annealed at 200ºC for 12 minutes and 20 minutes and let these samples are called as sample 1 and 2. The sample was annealed at about 100ºC for 2 hours to get phase-pure nanoparticles of CdS and the sample is known as sample A. Similarly, sample B is annealed at about 200°C for 2 hours and sample C is annealed at about 300°C for 2 hours. The structural and morphological characteristics of the CdS nanocrystals were studied with X-ray diffractometer and Scanning Electron Microscopy.

In order to synthesize the nanoparticles of doped CdS : Tm (Tm = Zn^{2+}, Mn^{2+}, Cu^{2+}) chemicals such as zinc

acetate, manganese acetate and copper acetate were taken as the precursor materials for doping. To obtain CdS: Zn^{2+}, 1 mol%, 2 mol% and 3 mol% of zinc acetate separately were added to the solution of cadmium acetate (Cd $(Ac)_2$) and thioacetamide (TAA) and was kept in the microwave oven. It was further processed similar to the processing of undoped CdS nanoparticles as explained above. Similarly, to synthesize CdS : Mn^{2+}, 1 mol%, 2 mol% and 3 mol% of manganese acetate were used, to obtain CdS : Cu^{2+} nanoparticles, 1 mol%, 2 mol%and 3 mol% of copper acetate were added separately to the solutions of cadmium acetate ($Cd(Ac)_2$) and thioacetamide (TAA).

1. Experimental

I. Powder XRD of Pure CdS nanoparticles

The figure (1) shows that the result of powder XRD of pure CdS nanoparticles and it contains cubic phase with a little hexagonal phase of CdS. Cubic CdS phase was most often found in synthesized colloidal CdS nanoparticles, but the macroscale phase of CdS is normally with the hexagonal structure (20). The hexagonal phase is more common in the solvothermal synthesis (22, 23). From the figure (1) it is evident, the coexistence of cubic and hexagonal phases of CdS nanoparticles (21). We also obtain cubic phase as well as hexagonal phase in the present system. The XRD pattern shows that there are three distinct peaks at three different angles.

All the XRD peaks are broadened and diffused and that is due to the nanocrystalline nature of particles. These nanocrystals have lesser lattice planes when it compared to bulk, which contributes to the broadening of the peaks in the diffraction pattern. This broadening of the peak is also due to the micro-straining of the crystal structure producing from defects like dislocation and twinning etc. XRD lines of broadened and diffused pattern are indicative of the small size of the CdS nanoparticles and the 'hkl' values as compared with the standard JCPDS file (5-0566). XRD peaks are found to be very broad which is indicating very fine size of the grains of the samples. In the figure(1) the XRD patterns exhibits prominent, broad peaks at 2 □ values of 26.60, 44.30 and 52.03 which could be indexed to scattering from (1 1 1), (2 2 0) and (3 1 1) and planes respectively of cubic CdS (24, 25). The grain size of the nanocrystalline CdS was calculated from the Scherrer's equation (26-28). The Scherrer's formula is given by: $D = 0.9\lambda/\beta Cos\theta$

Where D is the crystallite size in nm, λ is the wavelength of the X-rays (1.5406 Å), β is the full width at half maximum and θ is the diffraction peak angle. The results were shown in table 1 and 2.

From the figure (2) the XRD patterns of samples are annealed at different temperature for different time shows that with increasing the annealing time, the conversion of amorphous phase to crystalline phase has started. It seems that the effect of temperature on crystal phase formation is more predominance than annealing time. As the annealing time increases, the diffraction peaks become sharper and narrower, and the intensity increases which indicates that the intensification in crystal linty. Moreover from the figure (2) it is found that annealing time does not produce any change in the particle size of the nanoparticle. From the XRD pattern of sample A, sample B, sample C, it observed that the synthesized sample belongs to pure CdS phase.

From table (2), it is found that the peak width increases with the decreases of annealing temperature, which is an indication of particle size decrease with the decrease of annealing temperature and also peaks seems to be slightly shifted towards 26.68 which imply that the particle becomes more crystallized as the annealing

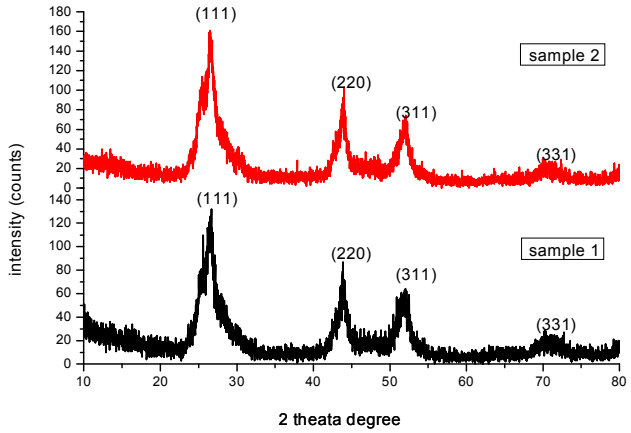

Fig. 1: XRD of Pure CdS Sample (1 and 2)

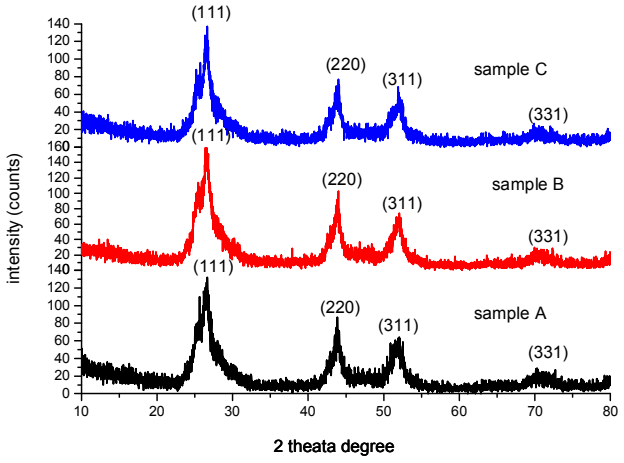

Fig. 2: XRD of Pure CdS Sample (A, B and 2)

temperature increases. The particle size is found to increase with increase in annealing temperature. In heating process when the particles are formed, they collide and either coalesce with each another to form a larger particle or coagulate. The process which occurs depends upon the temperature and available energy, that's why particle size increases with increasing temperature

Table 1: Particle size with diff. Annealing Time.

Name of the sample	Temperature	Annealing time (min)	Peak height (count)	Particle size (nm)
Sample 1	200^{0}C	12	121.32	14.06
Sample 2	200^{0}C	20	328.47	18.33

Table 2 : Particle size with diff. Annealing Temp.

Name of the sample	Temperature (^{0}C)	Annealing time (min)	Max Peak (2 theta)	Particle size (nm)
Sample A	100^{0}C	120	26.40	16.65
Sample B	200^{0}C	120	26.66	21.05
Sample C	300^{0}C	120	26.68	23.36

Table 3: Thermal parameters of pure and Zn^{2+} doped CdS

Material	TGA temp.(^{0}C)	DSC temp.(^{0}C)	DTA wt. loss(%)
Pure CdS	50 200 570	48	1 45
1mol%	100 - - 460 750	51.95 80.45 93.60 - -	- - 1 30
2 mol%	102 480 660	53.29	1 45
3 mol%	102 400 690	52.63 92.15	1 45

II Scanning Electron Microscopy (SEM)

The pure CdS nanoparticles are annealed at 100^{0}C for 120 minutes, 200^{0}C for 12 minutes and 200^{0}C for 20 minutes are termed as sample (A, 1 and 2) respectively. The SEM images were taken for the nanopowdered samples prepared by the present solvothermal method. Their SEM images are shown in figures (3, 4 and 5) respectively. From these figures it can be observed that the hexoganal phases of CdS nanoparticles are present (29, 30). The rough and spongy surface morphology is evident which makes it difficult to estimate the crystallite size due to agglomeration of the particles (31). The hexagonal and cubic structures were seen by all SEM images. The average particle size is found to be around 15.88 nm–18.79 nm. The particle size of the sample A, sample 1 and sample 2 are comparable with the particle size calculated by XRD. The grains have aggregated to form nanoclusters (32, 33).

The SEM images suggest size of grains to be much

Table 4: Thermal parameters of pure & CdS : Mn^{2+}

Material	TGA temp.(^{0}C)	DSC temp.(^{0}C)	DTA wt. loss(%)
Pure CdS	50 200 570	48	1 45
1 mol%	100 - - 370 620	- 56.67 - - -	- - 1 29
2mol%	102 460 690	59.62	1 45
3mol%	103 470 670	53.96 99.64	1 46

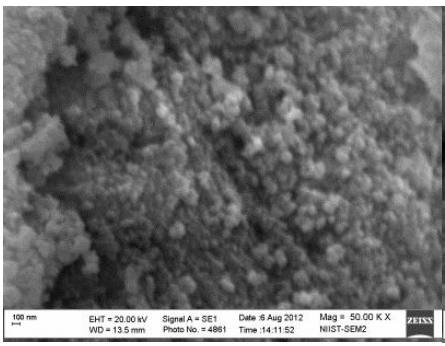

Fig. 3: (Sample A)

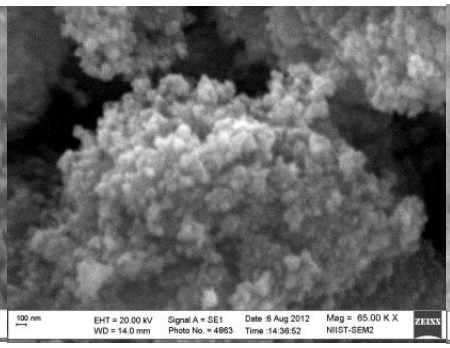

Fig. 4: (Sample 1)

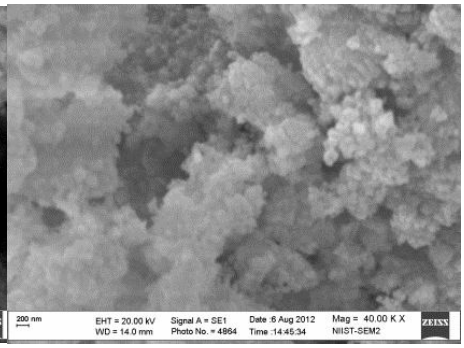

Fig. 5: (Sample 2)

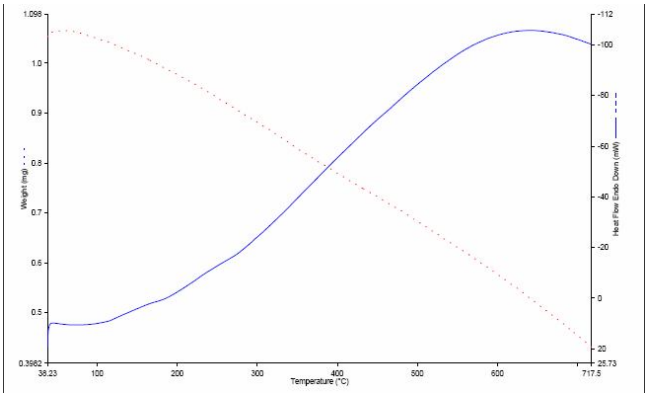

Fig. 6: TGA curve of Pure CdS

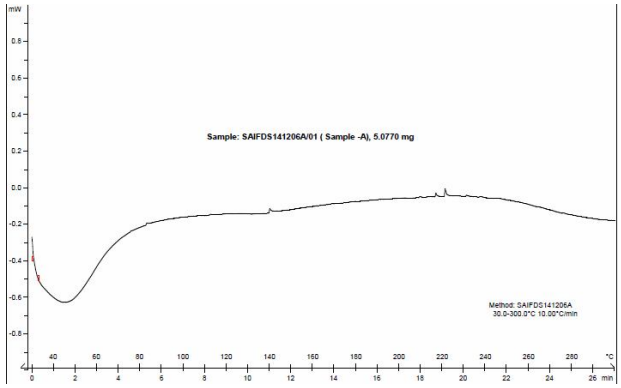

Fig. 7: DSC curve of Pure CdS

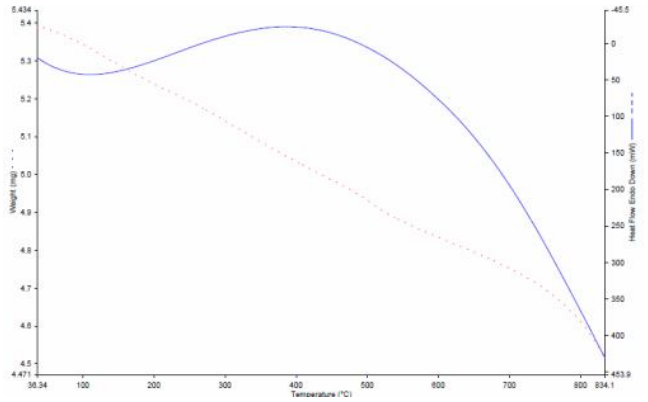

Fig. 8: TGA of Cds:Zn^{2+} (1 mol %)

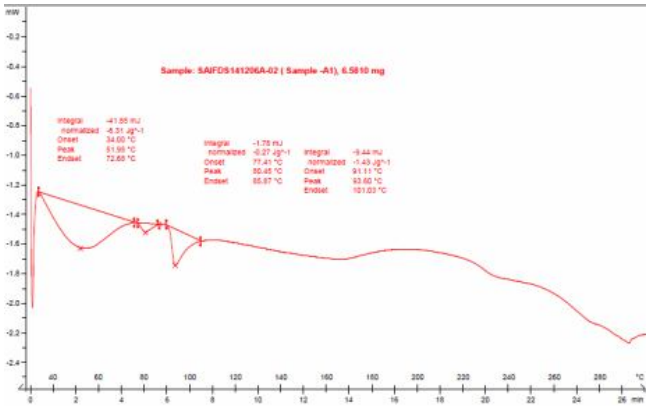

Fig. 9: DSC of Cds:Zn^{2+} (1 mol %)

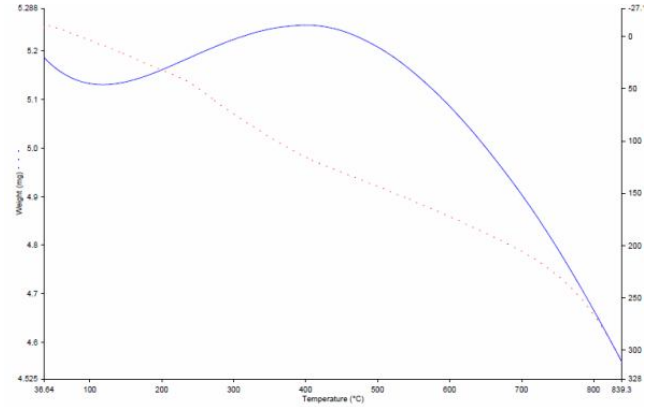

Fig. 10: TGA of Cds:Zn^{2+} (2 mol %)

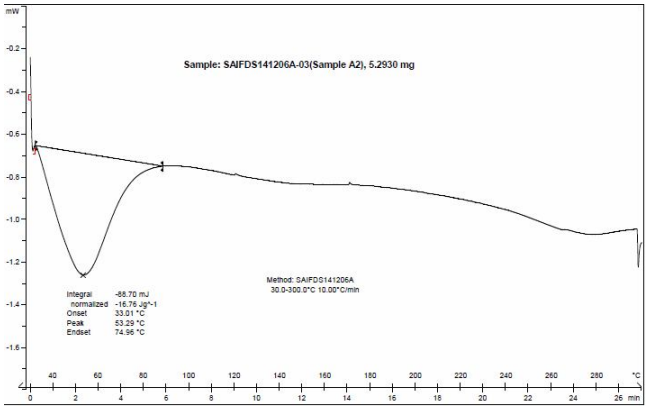

Fig. 11: DSC of Cds:Zn^{2+} (2 mol %)

larger. Further, while Scherrers calculation has suggest an increase in particle size with rise in annealing temperature, but SEM images indicate almost a reverse trend. Taking into account the above discrepancy and the fact that SEM analysis reveals formation of particles with different shapes and size, it seems appropriate to consider that the particles which appear in SEM images are in fact, grain agglomerates, which get fragmented with rise in annealing temperature. The morphology of all the samples are appeared uniform and the particle size is also low (34-36).

III. Thermal analysis of pure and doped CdS nanoparticles

Thermogravimetric analysis (TGA) is used to study the thermal decomposition of Pure CdS and CdS : Tm (Zn^{2+}, Mn^{2+}, Cu^{2+}) doped CdS nanoparticles. The synthesized specimens were heated from room temperature to 717.5^{0}C with an increment of 100^{0}C /min in air using simultaneous thermal system. The TGA analysis of Pure CdS is shown in the figure (6). In the weight loss is measured using TGA method and in the figure (6) the heat flow is denoted as endo down.

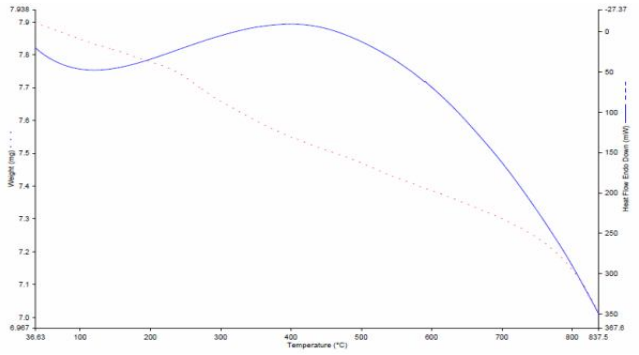

Fig. 12: TGA of Cds:Zn^{2+} (3 mol %)

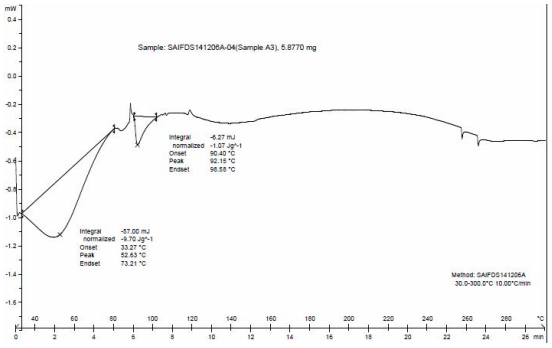

Fig. 13: TGA of Cds:Zn^{2+} (3 mol %)

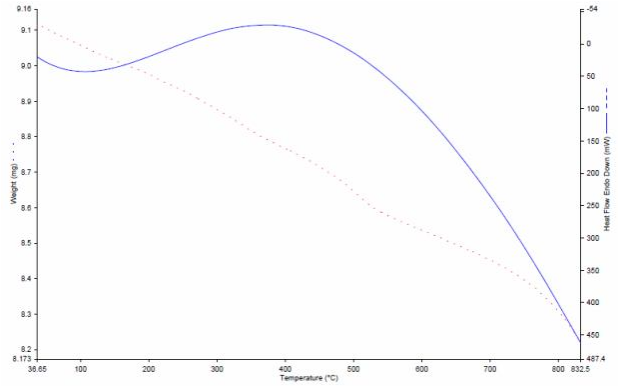

Fig. 14: TGA of Cds:Mn^{2+} (1 mol %)

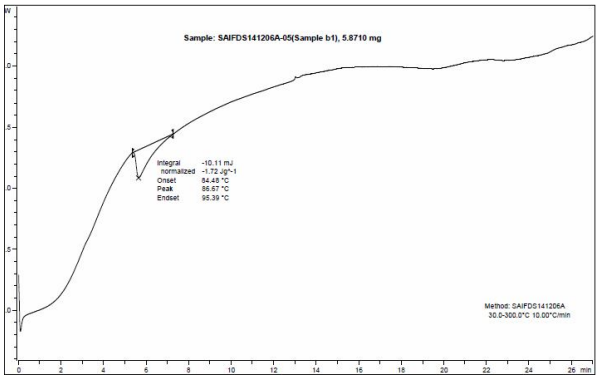

Fig. 15: DSC of Cds:Mn^{2+} (1 mol %)

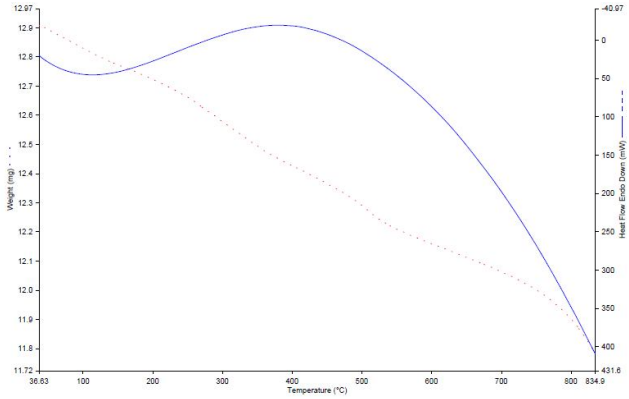

Fig. 16: TGA of Cds:Mn^{2+} (2 mol %)

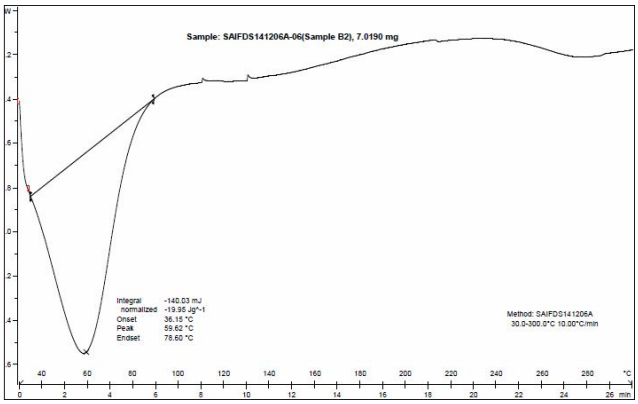

Fig. 17: DSC of Cds:Mn+2+ (2 mol %)

In the present investigation TGA of figure (6) shows that the sample is thermally stable with slight endothermic peak around 50^{0}C and other two at 80^{0}C and 93^{0}C. A very small weight loss below 100^{0}C can be generally attributed to the evaporation of absorbed water on the surface of the material. Due to this evaporation a very small weight loss is occurred in the material. Hence, the sample is thermally stable up to 100^{0}C. At 200^{0}C there is an exothermic peak has observed due to the evaporation of organic components on the surface of the material. So a weight loss of 1% is observed between 100^{0}C and 200^{0}C. It is followed by a major weight loss of around 45% between 200^{0}C to 570^{0}C and is ascribed to decomposition of covalently bound organic, particularly ethelylene glycol on the surface (37, 38).

The DSC curve of the pure CdS nanoparticles was also studied from 30^{0}C to 300^{0}C. Initially 6.58 mg was taken for the above study. figure (7) shows the DSC curve of the pure CdS nanoparticles. It is observed from the graph that, there is a peak around at 48^{0}C which is substantiates our earlier observation in TGA.

The TGA analysis of doped sample of 1mol% Cds: Zn^{2+}, is shown in the figure (8). Thermogravimetric analysis (TGA) trace is shown from 36.34^{0}C to 834.1^{0}C

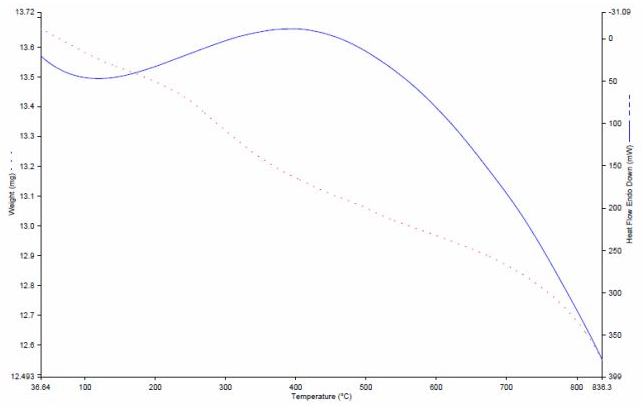

Fig. 18: TGA of Cds:Mn^{2+} (3 mol %)

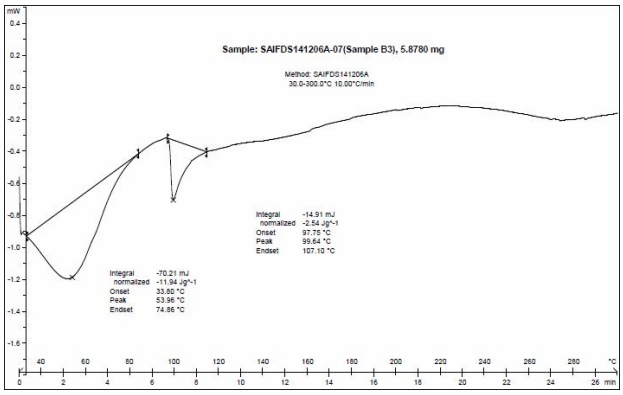

Fig. 19: DSC of Cds:Mn^{2+} (3 mol %)

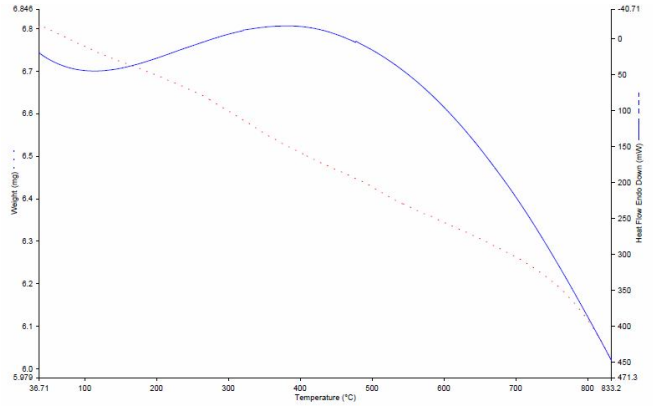

Fig. 20: TGA of Cds:Cu^{2+} (1 mol %)

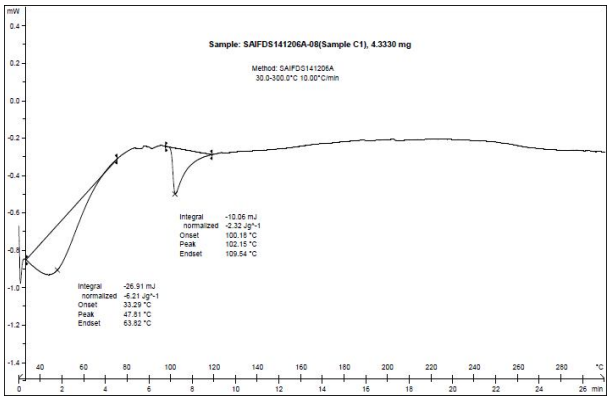

Fig. 21: DSC of Cds:Cu^{2+}(1 mol %)

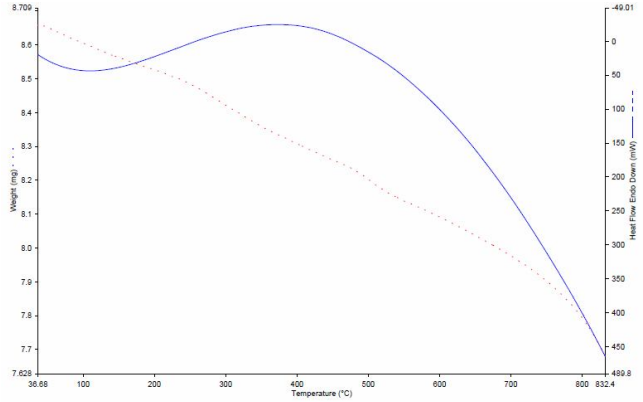

Fig. 22: TGA of Cds:Cu^{2+}(2 mol %)

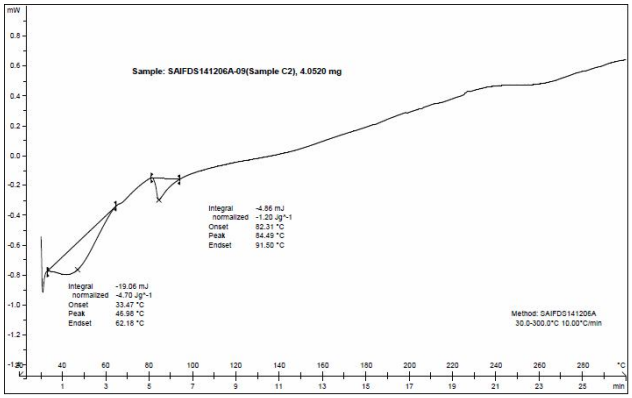

Fig. 23: DSC of Cds:Cu^{2+}(2 mol %)

and in this TGA curve around 100^{0}C an endothermic curve is present. It represents the presence of water molecules on the surface of the material and it is evaporated at that temperature. There is an another exothermic peak has observed at 460^{0}Cand it can be generally attributed to the evaporation of organic components on the surface of the material. The TGA curve is also exhibit 35% of weight loss in the doped CdS nanoparticles. It is clearly proved that, when the concentration of the dopant has increased the thermal stability for the nanoparticles also improved significantly as higher as doping concentration of pure CdS in the TGA. It might be related to the combination of CdS nano crystalline in the organic compounds, which yielded stronger binding force due to the interaction between CdS nanoparticles and lone pair electrons of N atom in the organic backbone (39, 40). It is followed by a major weight loss at around 750^{0}C (5.301mg to 4.525mg, *i.e.,* around 0.776mg) there is an endothermic peak and is ascribed to decomposition of covalently bound organic, particularly sulphur gas molecules on the surface has gone out. The TGA analysis of Zn^{2+} doped CdS nanoparticles

Table 5 : Thermal parameters of pure & CdS : Mn^{2+}

Material	TGA temp.(^{0}C)	DSC temp.(^{0}C)	DTA wt. loss(%)
Pure CdS	50 200 570	48	1 45
1mol%	100 - - 460 650	47.81 - 102.15 - -	- - 1 30
2mol%	101 480 680	46.98 84.49	1 47
3mol%	103 490 690	54.62 85.61	1 45

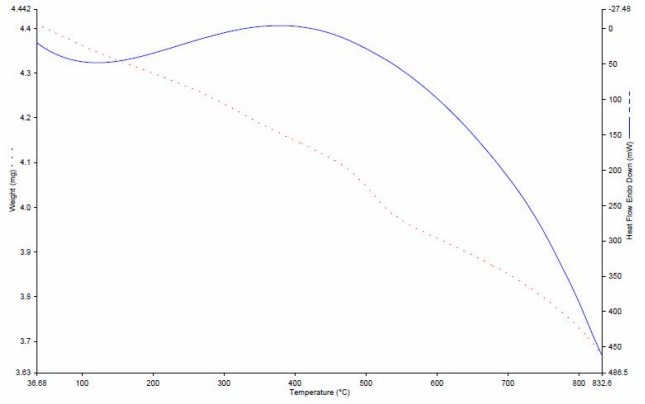

Fig. 24: TGA of Cds:Cu^{2+} (3 mol %)

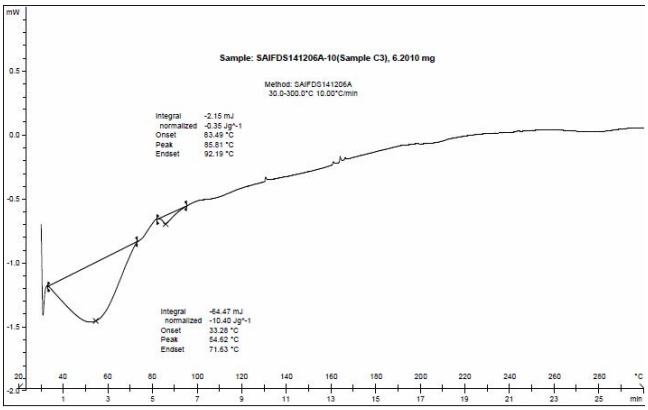

Fig. 25: DSC of CdS:Cu^{2+} (3 mol %)

for 2 mol% and 3mol% are shown in figures (10 and 12) respectively.

From the figure (9) the DSC curve also clearly depicts three peaks at 51.95^{0}C, 80.45^{0}C and 93.60^{0}C. All these lower peaks attribute the change of phase from amorphous to crystalline nature of the Zn^{2+} doped nanopartticle and the peak at 93.60^{0}C may be attributed to the loss of water molecule present on the surface of the material. It also exhibits a peak around 240^{0}C and the analysis is observed up to 300^{0}C only. The DSC analysis curves are shown in figures (11 and 13) respectively.

From the table (3) it gives that the various thermal parameters of the pure and Zn^{2+} doped CdS nanoparticles. In the table (3) it is clearly understood that the TGA and DSC temperatures explains the thermal behaviour of the pure and doped nanoparticles. The increase in the doping concentration are slightly altered the endothermic peaks of the samples. The major weight loss peak is shifted from 46^{0}C to 480^{0}C and the second peak is shifted to 660^{0}C to 690^{0}C when the doping concentration increases to 2 mol% to 3 mol%. It might be related to the combination of CdS nanocrystalline in the organic compounds, which yielded stronger binding force due to the interaction between CdS nanoparticles and lone pair electrons of N atom in the organic backbone (41, 42). It is followed by a major weight loss up to 660^{0}C (5.18mg to 4.56mg, *i.e.,* around 0.62mg) there is an endothermic peak and is ascribed to decomposition of covalently bound organic, particularly sulphur gas molecules on the surface has gone out.

The TGA and DSC curves of Mn^{2+} doped and Cu^{2+} doped with 1 mol%, 2 mol% and 3 mol% are shown in figures (14 to 25). The corresponding thermal parameters are given in table (4 and 5) respectively. The major weight loss, obtained in the second stage is due to the elimination of ligand present in the Cd-Mn complex and the observed weight loss is about 45%. At higher temperature (370^{0}C to 490°C), the curve shows a shoulder peak, corresponding to a slight weight loss. The DTA curves of this complex exhibit a sharp and somewhat broad enxothermic peak in the temperature regions 380°C and 832°C respectively. The broad endothermic nature of these DTA peak implies some kind of phase change associated with the absorption of required latent heat. The TGA steps, corresponding to decomposition of ligands of the complex involving sudden weight loss, are accompanied by relatively sharp peak in DTA. At the DTA peak corresponding 170 to the phase change of the complex prior to any actual disassociation, the TGA curve obviously exhibit no weight loss steps.

There won't be much aprectiable change in the peak temperatures of the dopants. The major weight loss, obtained in the second stage is due to the elimination of ligand present in the Cd:Mn and Cd:Cu complex and the observed weight loss is about 45%. At higher temperature (370^{0}C to 490°C), the curve shows a shoulder peak,

corresponding to a slight weight loss. The DTA curves of this complex exhibit a sharp and somewhat broad enxothermic peak in the temperature regions 380°C and 832°C respectively. The broad endothermic nature of these DTA peak implies some kind of phase change associated with the absorption of required latent heat.

References

Alivisatos, A.P. and J. Phys (1996). *Chem.,* **100(31)** : 3226.

Alivisatos, A. P. (1996). *J. Phys. Chem.,* **100** : 13226.

Balaz, P., E. Boldizarova, E. Godocikova and J. Briancin (2003). *Mates. Let.,* **57** : 1585-1589.

Brus, L. and J. Phys (1998). *Chem. Solids,* **59(4)** : 459.

Cahill, C. L., B. Gugliotta and J . B. Parise (1998). *Chem. Commun*., **16** : 1715.

Cao, B.L.,Y. Jiang , C. Wang, W.H. Wang, L.Z. Li, M. Niu, W.J. Zhang, Y.Q. Li and S.T. Lee (2007). *Adv. Funet Mater,* **17** : 1501.

Castanon, G. A. Martinez, M. G. Sanchez Loredo, J. R. Martinez Mendoza and Facundo Ruiz (2005). vol.1.

Chory, C. Braglik, D. Buchold, M. Schmitt, W. KIefe, C. Heske, C. Kumpf, O. Fuchs, L. Weinhardt, A. Stahl, E. Umbanch,M. Lentze, J. Geurts and G. Muller (2003). *Chem. Phy. Lett.,* **379** : 443-451.

Cullity, B.D. (1967). Elements of X-Ray Diffraction, Addison-Wesley Publishing Co., Inc.,.

Deng, J.G., X.B. Ding, W.C Zhang, Y.X. Peng, J.H Wang, X.P. long, P. Li and S.C. Chan (2002). *Polymer,* **43** : 2179.

De la, M., L. Olvera, A. Madonado, R. Asomoza, Konagai and M. Asomoza (1998).

Demazeau, G. (1999) . *J. Mater. Chem*., **9** : 10.

Derfus, A.M., W.C.W. Chan and S.N. Bhatia (2004). *Adv. Mater,* **16** : 961.

Dimitrov, R. I., N. Moldovanska and I. K. Bonev (2002). *Cds Oxi,* **385** : 41-49.

Duan, X.F., Y. Huang, R. Agarwal and C.M. Lieber (2003). *Nature,* **421** : 241.

Guo, G. C., R. M. W. Kwok and T. C. W. Mak (1997). *Inorg.Chem. Soc.,* **36** : 2475.

Henglein, A. (1989). *Chem. Rev,* **89** : 1861.

Kamata, K., S. Matsumoto, P. Souleite and B. W Wessels (1988).

Kamat, P.V., K. Murakoshi, Y. Wada and S.Yanagida (2000). In: H.S.Nalwa (Ed.), Handbook of Nanostructured Materials and Nanotechnology, Academic Press, San Diego, p.129.

Li, Y. H. Liao, Y. Fan, L. Li and Y. Qian (1999). *Mater. Chem. Phys*., **58** : 87.

Li, Y., H. Liao, Y. Ding, Y. Fan, Y.Zhang and Y. Qian (1989). *Inorg. Chem*., **38** : 1283.

Mathew, X., J. P. Enriquez, A. Romeo and A.N. Tiwari (2004) . *Sol Energy,* **77** : 831.

Masui, T., H. Hirai and N. Imanaka (2002). *J. Materials Science Lett.,* **21**: 489.

Murray, C. B., D. J. Norris and M. G. Bawendl (1993). *J Am.Chem. Soc.,* **15** : 8706.

Meron, T. and G. Markovich (2005). *J. Phys. Chem.,* **109** : 20232.

Pawar, S.G., M. A. Chougule, P.R Godse, D. M. Jundale, S. A. Pawar, B. T. Raut and V. B. Patil (2011). *J. Nano. Ele. Phy.* **3** : 185-192.

Rao, B. Sreenivasa, B. Rajesh Kumar, V. Rajagopal Reddy and T. Subba Rao (2011). *Chl. Let.,* **8** : 177-185.

Sabha, A.Aneeqa, Saadat Anwar Siddiqi and Salamat Ali (2010). *Wld. Acdmy. of Scin. Engg and Tech,* **45**.

Shao, M., Q. Li, L. Kong, W. Yu and Y. Qian (2003), *J. Phys. Chem. Solids* **64**, 1147.

Ramnath, B., B. Rajeev Kumar, K. Veeragopal Beddy and T. Subbayler (2011). *Chl. Let.,* **8** : 177-185.

Sharma, T.P., D. Patdar, N .S. Saxena and K .Sharma (2005). *Ind. J. Pure & Appl. Phys.,* **44** : 125.

Scgur, M. and W. Bensch (1998). *Z. Anorg. Allg. Che.,* **624**: 310.

Schur, M., H. Rijnberk and C. Nather (1998). *Polyhedron,* **18:** 101.

Thambidurai, M., N. Muthukumarasamy, S. Agilan, N. Murugan, N. Sabari Arul, S. Vasantha and R. Balasundaraprabhu (2010). *Solid State Scin.,* **12** : 1554-1559.

Trindade, T., P.O.'Brien and N.L. Pickett (2001). *Chem, Mater,* **13**: 3843.

Venugopal, P. and K. Ravichandran (2013). *Adv. Mat. Lett.,* **4(1)** : 200-206.

Wang, W., I .Germanenko and M. Samy El-Shall (2002). *Chem. Mater.,* **14**: 3028.

Wang, W., Z.I Germanenko and M.S.E. Shall (2002). *Chem. Mater,* **14** : 3028.

Weller, H. and Angew (1993). *Chem.* **105**: 43.

Xie, Y., Y. Qian,W. Wang, S. Zhang and Y. Zhang (1996). *Science,* **272** : 1926.

Yu, S., J. Yang, Y. Wu, Z. Han, J. Lu, Y. Xie and Y. Qian (1999). *Mater. Chem.,* **9** : 1283.